On the Estimation of High-Dimensional Surrogate Models of Steady-State of Plant-wide Processes Characteristics

Article *in* Computers & Chemical Engineering · February 2018
DOI: 10.1016/j.compchemeng.2018.02.014

CITATIONS
0

READS
34

2 authors:

Anh Phong Tran
Northeastern University
4 PUBLICATIONS **1** CITATION
SEE PROFILE

Christos Georgakis
Tufts University
199 PUBLICATIONS **4,127** CITATIONS
SEE PROFILE

Computers and Chemical Engineering 000 (2018) 1–13

Contents lists available at ScienceDirect

Computers and Chemical Engineering

journal homepage: www.elsevier.com/locate/compchemeng

On the estimation of high-dimensional surrogate models of steady-state of plant-wide processes characteristics

Anh Phong Tran[a], Christos Georgakis[b,*]

[a] Department of Chemical Engineering, Northeastern University, Boston, MA 02115, USA
[b] Department of Chemical and Biological Engineering, Tufts University, Medford, MA 02155, USA

ARTICLE INFO

Article history:
Received 20 September 2017
Revised 15 February 2018
Accepted 17 February 2018
Available online xxx

Keywords:
Surrogate model
Metamodel
Process operability
Process optimization
Design of experiments
Plant-wide control
Net-elastic regularization

ABSTRACT

This work generalizes a preliminary investigation (Georgakis and Li, 2010) in which we examined the use of Response Surface Methodology (RSM) for the estimation of surrogate models as accurate approximations of high-dimensional knowledge-driven models. Three processes are examined with higher complexity than before, accounting for a much larger number of input and output variables. The surrogate models obtained are used to analyze several steady-state plant-wide characteristics. In all processes, the knowledge-driven model is a dynamic simulation with a plant-wide control structure of multiple SISO controllers. This type of controller proves to not be robust enough in its stability characteristics to enable substantial changes in the set-points. The net-elastic regularization is successfully used for the estimation of the metamodel parameters, avoiding overfitting and eliminating insignificant terms. Cross validation is used to compare and evaluate the relative accuracy of the quadratic and cubic models.

1. Introduction

Increasingly detailed knowledge-driven plant-wide models can be developed through popular simulation tools like ASPEN Plus, ASPEN Dynamics, gPROMS or other process simulation software. These detailed steady state and dynamic models are commonly used off-line to study different characteristics of a process, such as in its design. However, once the process has been designed and/or built, using these models to study operability characteristics, real time optimization, or control or scheduling tasks can be a challenging task. Such detailed models may not be suitable for on-line use because they are often too detailed and computationally intensive for the intended on-line purposes. For example, their use in optimization tools such as BARON (Sahinidis, 1996) and IPOPT (Biegler and Zavala, 2009) are quite cumbersome. Simplified versions of such detailed models, also referred to as metamodels or surrogate models, present an attractive alternative to solving such computational difficulties. However, there remain open questions about which metamodel basis functions to use, the sampling methods to be employed, how the parameters should be estimated, and where these metamodels can be effectively applied. Only steady-state metamodels or surrogate models are considered in the present paper, similarly to the majority of the existing literature.

Interest in developing reduced-size surrogate models of detailed knowledge-driven models has substantially increased in recent years. Banerjee and Ierapetritou (2006) described the use of reduced models in accurately predicting the behavior of complicated reactive flow systems involving hundreds of species. By reducing the model complexity over a specific range of conditions, the computationally expensive task of accounting for the kinetics of hundreds of chemical species is significantly reduced. Caballero and Grossmann (2008) introduced an algorithm using Kriging metamodels for the optimization of modular process simulators. Henao and Maravelias (2010) developed surrogate models based on artificial neural networks (ANN) to accurately approximate ASPEN first principles models of pumps, compressors, turbines and flash vessels. The authors point out that superstructure optimization for complex process synthesis tasks is often impractical, and that this typically results in non-convex Mixed-Integer Nonlinear Programs (MINLP) that are hard to solve. Fahmi and Cremaschi (2012) developed surrogate models using ANN in a biodiesel product plant simulation, an approach for which an adaptive sampling method was developed by Eason and Cremaschi (2014). Zhang and Sahinidis (2012) built surrogate models of a carbon sequestration system using a polynomial chaos expansion. In this study, the variations in porosity and permeability were

* Corresponding author.
E-mail address: christos.georgakis@tufts.edu (C. Georgakis).

https://doi.org/10.1016/j.compchemeng.2018.02.014
0098-1354/

studied and a stepwise regression was used to reduce the size of the resulting metamodel.

On the global optimization side, Müller et al. (2013) and Müller and Shoemaker (2014) introduced the SO–MI algorithm to solve computationally expensive mixed-integer black-box global optimization problems as well as the influence of ensemble surrogate models and the sampling strategy for such problems. Cozad et al. (2014) implemented the automated learning of algebraic models for optimization (ALAMO) methodology to describe a flash drum and a carbon capture absorber. The global optimization algorithms ANTIGONE for continuous/integer optimization of nonlinear equations and ARGONAUT for constrained grey-box problems were proposed by Misener and Floudas (2014) and Boukouvala and Floudas (2017), respectively. Boukouvala et al. (2017) has recently introduced a new methodology that addresses the global optimization of general constrained grey-box problems that combines various sampling techniques, multiple types of functional forms, and various deterministic optimization methods.

Furthermore, our research group has demonstrated the effectiveness of the Design of Experiment (DoE) Methodology and the corresponding Response Surface Methodology (RSM) to develop surrogate models for the study of nonlinear process characteristics (Georgakis and Li, 2010). We have also introduced generalizations of the classical DoE approach to allow time-varying inputs by introducing the Design of Dynamic Experiment (DoDE) approach (Georgakis, 2013). Similarly, the Dynamic Response Surface Methodology (DRSM) (Klebanov and Georgakis, 2016) is a generalization of the RSM model to account for time-varying output measurements. Though not exhaustive, the above list of publications, related to the development and use of surrogate models, attests to the importance of the subject. The main focus in the development of metamodels relies on the choice of a basis function, the sampling method, and the regression technique used for the estimation of the model parameters.

Various functional bases have been proposed in the development of surrogate models. A polynomial functional basis is often considered for its simple form. Kriging models have been proposed as a stochastic approach to estimate nonlinear models, but are also more difficult to estimate. Radius basis function (RBF) can be used to build networks analogous to artificial neural networks (ANNs). Multivariate adaptive regression splines (MARS) can adaptively fit a model by a series of piecewise linear regressions (Jin et al., 2001; Wang and Shan, 2007). Additionally, support vector machines (SVMs) have been extensively studied for classification and regression applications, especially in the domain of machine learning (Noble, 2006). Often, there is no *a priori* knowledge on which basis function is ideal for a given application.

In the estimation of surrogate models for chemical processes, it is often necessary to limit the number of data points that need to be calculated when using the detailed simulation models. Monte Carlo (MC) and Quasi-Monte Carlo sampling methods are considered too slow to converge for large dimensional problems, and were not considered in this work. Instead, the widely-used D-optimal Design of Experiments (DoE) methodology is used for its abilities to handle higher-order polynomials and control the number of detailed simulations required. More details on the functional bases and sampling methods can be found in related reviews (Bhosekar and Ierapetritou, 2017; Jin et al., 2001; Wang and Shan, 2007).

In the estimation of the metamodel parameters, the regression technique to be used has a large impact on the accuracy of the metamodel. The simplest and most commonly used method is the ordinary least-squares (OLS) that aims to minimize the least-squares error between the data and the metamodel predictions. However, its simplicity also leads to issues such as poor performance in the presence of collinearity and sensitivity to noise and outliers. A preferred alternative is the use of stepwise regression (SWR) that removes insignificant predictors. Since SWR performs and compares several OLS tasks with various subsets of the metamodel parameters, the modeling task is time consuming and becomes a challenge with high dimensional metamodels where there are many parameters. To minimize issues related to overfitting, regularized least-square regressions have gained popularity. While OLS attempts to minimize the squared error between the data and the model, the regularized least-squares approach introduces one additional penalty term linked to the model parameters. The regularized error form shown in Eq. (1) contains the least-square term, and adds a regularization term. Here t_n represents the data and $w^T\varphi(x_n)$ the model's prediction with w denoting the fitted coefficients and φ the basis function. The second term is a penalty for the size of the model parameters while the λ constant affects the magnitude of regularization imposed. This function is minimized with respect to the parameter values to be estimated.

$$\frac{1}{2}\sum_{n=1}^{N}\left\{t_n - w^T\phi(x_n)\right\}^2 + \frac{\lambda}{2}\sum_{j=1}^{M}\left|w_j\right|^q \tag{1}$$

In the case $q=1$, implying an L_1 norm, the expression becomes the LASSO regularization technique that is widely used for its ability to drive insignificant parameters to zero and give a sparse model when λ is sufficiently large (Tibshirani, 1996). In general, the best value for λ is estimated through cross-validation. When $q=2$, corresponding to an L_2 norm, the penalty term is quadratic, and the approach corresponds to the Tikhonov regularization that has many applications when dealing with ill-posed problems and noisy data. Both L_1 and L_2 penalty terms limit the magnitude of the coefficients, and thus control the overfitting of the data which degrades the predictive performance of the fitted model. More recently, the net-elastic regularization proved to be effective by combining these L_1 and L_2 penalty terms (Zou and Hastie, 2005).

In the following sections, we show how the use of the net-elastic regularization, combined with quadratic or cubic D-optimal DoE designs, yields accurate metamodels. The D-optimal or one of many other optimal DoE designs offer an efficient way for the selection of the conditions at which the detailed simulations are evaluated. Our specific interest here is to consider high-dimensional problems related to three realistic process simulations producing ethyl benzene, mono-isopropyl amine and the Tennessee Eastman processes. Extending on the findings reported in Georgakis and Li (2010), this work addresses:

- The applicability of D-optimal designs to develop surrogate models of much larger size problems than those previously considered. The problem size is defined primarily by the number of inputs and outputs.
- The use of the obtained surrogate models to easily perform process calculations that would have been challenging, if not impossible, using the detailed models.
- The implementation of the net-elastic regularization approach for the estimation of the parameters of the surrogate model. In comparison to step-wide regression, this approach addresses possible overfitting, reduces model complexity, and reduces estimation times

2. Methodology

2.1. Model selection and sampling method

The simplest design of experiment (DoE) model often considered contains only the linear and interaction terms for which the inputs need to take values in only two levels to estimate the

Please cite this article as: A.P. Tran, C. Georgakis, On the estimation of high-dimensional surrogate models of steady-state of plant-wide processes characteristics, Computers and Chemical Engineering (2018), https://doi.org/10.1016/j.compchemeng.2018.02.014

model's coefficients:

$$y = \beta_0 + \sum_{i=1}^{n} \beta_i u_i + \sum_{i=1}^{n} \sum_{j>i}^{n} \beta_{ij} u_i u_j \quad (2)$$

By considering three levels for each process input, quadratic terms can be estimated to further describe the process nonlinearities:

$$y = \beta_0 + \sum_{i=1}^{n} \beta_i u_i + \sum_{i=1}^{n} \sum_{j>i}^{n} \beta_{ij} u_i u_j + \sum_{i=1}^{n} \beta_i u_i^2 \quad (3)$$

In our preliminary study (Georgakis and Li, 2010), we showed that a model of the simple form of Eq. (3) could estimate the nonlinearities of a plant-wide process reasonably well. In the present work, the input sets under consideration are substantially more numerous and demonstrate the scalability of this approach. At the same time, wider input ranges are examined, and higher order nonlinearities are explored as a way of improving the accuracy of the surrogate model. In particular, cubic RSM models, who include cubic and third-order interaction terms, are explored throughout this work:

$$y = \beta_0 + \sum_{i=1}^{n} \beta_i u_i + \sum_{i=1}^{n} \sum_{j>i}^{n} \beta_{ij} u_i u_j + \sum_{i=1}^{n} \beta_{ii} u_{ii}^2 + \sum_{i=1}^{n} \sum_{j>i}^{n} \sum_{k>j}^{n} \beta_{ijk} u_i u_j u_k + \sum_{i=1}^{n} \sum_{j>i}^{n} \beta_{ij} u_i^2 u_j + \sum_{i=1}^{n} \beta_{iii} u_{ii}^3 \quad (4)$$

The investigation of plant-wide processes with a high number of input variables necessitated particular attention on how to efficiently sample the design space. Using techniques such as full factorial or fractional factorial designs with three or four levels per inputs substantially increase the amount of data to be collected. In the case of a full factorial design for the estimation of the coefficients in Eq. (4), one needs 4^n calculations of the detailed model, where n is the number of inputs. This is equal to 16,384 data points to be collected when using 7 inputs and 262,144 data points for 9 inputs. Using a fractional factorial design can help reduce this excessively large sample size, but the amount of calculations of the detailed model still remains high enough that it can easily offset the benefits of using the metamodels instead of the detailed model. Other designs such as central composite designs (CCD) or Box-Behnken are effective for many applications, but were not derived to handle nonlinearities of degree order higher than 2.

The use of optimal designs (such as the D-optimal one) is the method of choice in this work due to their ability to only select as many points as needed for the appropriate estimation of the intended model's parameters. Because we do not know *a priori* whether a quadratic or cubic model is sufficient in providing the desired metamodel accuracy, an evolutionary approach should be used. First, the simplest model that appears reasonable is estimated; for example, a quadratic one. If the model is not sufficiently accurate, the number of detailed simulations used for its estimation can then be used for the estimation of a cubic model. This is achieved by appending to the existing enough additional runs to be able to estimate the increased number of parameters of the cubic model. In this work, the data points are always larger than the number of estimated parameters to avoid overfitting and ill-posedness issues.

2.2. Specification of the design space

For a given process, there are often specifications for the range of operations that should be represented in the surrogate model. In most DoE applications, the input variables are defined as differences from an initial operating point. They are made dimensionless with the expected positive or negative deviations from this reference point. They are then called *coded* variables with the initial operating point having a coded value equal to zero. Assuming that the range of interest is symmetric around this point, the maximum input value is coded to +1 and the minimum to −1. A substantial difficulty arises when one uses a dynamic simulation to calculate the steady-state data, needed to estimate the surrogate model. As the inputs are changed to the desired new values and the dynamic simulation stated, a new sampled data point can only be collected if the plant-wide control strategy is stable at the new steady-state. This problem has presented a serious challenge in our study with all three of the processes examined, especially when the values of more than one input were changed simultaneously. This reveals a weakness of the plant-wide control structure embedded in the simulations used. It points to the urgent need for more robust plant-wide control structures, especially if one wishes to integrate the tasks of plant-wide control and process scheduling. For our study, the above limitation restricted us from examining wider input ranges.

In searching for a suitable metamodel for the processes explored, the initial use of a quadratic D-optimal design was found to be particularly suitable. The data points for a D-optimal design often lie at the boundaries of the design space, and thus allow us to have a sense of which input conditions cause instability in the plant-wide control strategy. The ranges of each input can then be either increased or decreased until the largest possible stable design space is found. It is also important to note that the boundaries of stability often not only depend on the minimum and maximum stable values for the individual inputs, but also on the combined extreme values of more than one input. While not explored in this work, more elaborate linear or nonlinear constraints than the boundaries of a hypercube are needed to define the largest possible input space for which the plant-wide controller is stable. Such constraints are typically not easy to identify. If they can be determined, they can be incorporated as part of the D-optimal design.

2.3. Regression of the metamodel parameters

The metamodel parameters are regressed using the net-elastic regularization:

$$\min_{(\beta_0,\beta)} \frac{1}{2N} \sum_{i=1}^{N} \left(y_i - \beta_0 - x_i^T \beta\right)^2 + \lambda \left[\frac{(1-\alpha)\|\beta\|_2^2}{2} + \alpha \|\beta\|_1 \right] \quad (5)$$

Here the vector $\boldsymbol{\beta}$ represents the model parameters. The *glmnet* package is used and the algorithm is based on a cyclical coordinate descent algorithm (Qian et al., 2013). The optimal value of λ is automatically fitted through repeated cross-validation calculations for a specified value of α. A k-fold cross validation with a $k = 10$ was used in this work. The parameter α is then varied in a grid-like fashion between 0 and 1 and the value of α leading to the lowest cross-validation error is then kept. Stepwise regression was initially considered, but we noted large regression times when trying to estimate values for a few hundred model parameters.

2.4. Model validation

Additional points are calculated with random sets of input values each drawn from a uniform distribution that spans from −1 to 1. The root-mean-square error (RMSE) is then calculated to validate the accuracy of the developed models:

$$RMSE = \sqrt{\frac{\sum_{i=1}^{m} \left(y_i - \hat{y}_i\right)^2}{m}} \quad (6)$$

Given the large number and variety of output variables modeled for the three processes (each with different units), there was

Please cite this article as: A.P. Tran, C. Georgakis, On the estimation of high-dimensional surrogate models of steady-state of plant-wide processes characteristics, Computers and Chemical Engineering (2018), https://doi.org/10.1016/j.compchemeng.2018.02.014

a need to make this quantity dimensionless. This was achieved by dividing this quantity by the respective magnitude of the output range of each variable over all data to form a normalized RMSE:

$$NRMSE = \frac{100\%}{|\mathrm{Max(data)} - \mathrm{Min(data)}|}\sqrt{\frac{\sum_{i=1}^{m}\left(y_i - \hat{y}_i\right)^2}{m}} \tag{7}$$

A conservatively large number of runs was used for both in the estimation of the model parameters and in the cross-validation test to ensure that the metamodels estimated were as accurate as possible. For the parameter estimation, we used three times as many data points as the number of parameters. In the cross validation, 1000 runs were used. In cases where the detailed simulation takes considerable time to generate a single data point, the set of runs for estimating the metamodel can be drastically reduced to as many runs as there are model parameters, plus a few additional points to limit overfitting.

2.5. Uses of surrogate models

The three plant-wide process simulations that are explored in this work are:

i. The Tennessee Eastman process;
ii. An ethyl benzene process and;
iii. A mono-isopropyl amine process.

For each example, the dynamic simulation with the reported plant-wide controller is used and the set points to the controllers are varied within a given input space. The plant-wide control structures active in two of these processes have been designed by Luyben (2012). There are obvious differences between any two of these three processes, in the number and type of units involved, the number and type of the recycle steams and the types of nonlinearities in the behavior of the individual units. For this reason, the detailed examination of the performance of the proposed methodology in the above processes provides extra confidence that the initial success reported in our earlier work (Georgakis and Li, 2010) has much greater applicability to other processes and the development of surrogate models involving a much larger number of process inputs. Besides elucidating the development of the metamodels, we also present examples on how these models can easily be used to provide process insights that would have been difficult or impossible to achieve through the detailed simulations. The possible usages of these surrogate models presented here include calculations on heat integration, process operability, process optimization and insights onto the snowball effect. These uses are made possible by the ability of the surrogate models to succinctly capture the dominant input-output relationships in a simple functional form. The usage of such metamodels is envisioned to be much wider than presented here.

3. Tennessee Eastman (TE) process

3.1. Process description

The Tennessee Eastman process has been extensively studied and is often seen as a benchmark in the study of plant-wide control structures. It was first introduced in 1993 (Downs and Vogel, 1993), and a number of control structures have been proposed since then (Larsson et al., 2001; Lyman and Georgakis, 1995; Ricker, 1996). An adaptation of the control structure from Ricker (1996) for the base case (mode 1) is used here to alleviate compatibility issues with the more recent versions of MATLAB code used for its simulation (Bathelt et al., 2015).

The schematic of the process is shown in Fig. 1. It involves eight components: four reactants (A, B, C and E), two desired products (G and H), one inert B, and a byproduct F. The reactions relating these components are:

$$\begin{aligned} &A(g) + C(g) + D(g) \rightarrow G(l)\\ &A(g) + C(g) + E(g) \rightarrow H(l)\\ &A(g) + E(g) \rightarrow F(l)\\ &3D(g) \rightarrow 2F(l) \end{aligned} \tag{8}$$

The original FORTRAN code aimed to hide the inner details of the process kinetics and related details about the other process units. The initial information about the reactions that was communicated was quite limited, aiming to indicate that detailed knowledge-driven model is not available for the process. Nevertheless, we will assume that such a model is at hand and we will investigate whether an accurate metamodel can be estimated. In this process, there are five unit operations: a reactor where the liquid products are formed from the gaseous reactions, a product condenser, a vapor-liquid separator recycling the vapor phase to the reactor, a compressor, and a stripper. Mode 1 of this process has a base case that produces the two products G and H in a 50/50 mass ratio.

3.2. Estimation of the surrogate models

For the calculation of the response surface models, 9 controller set points were varied and are listed in Table 1. The remaining controller set points were kept constant: the steam and recycle valve positions were left closed, and the agitator was kept at 100%. It is important to note that the design space defined by the minimum and maximum values of the inputs used in the development of the surrogate models is only a subset of the input space that would have been of interest. This restriction to a subspace of stable steady states is a limitation imposed by the plant-wide control strategy in the process simulation used. A change of the input values outside this restricted input space might result in an unstable operation with the current controller, and thus the corresponding steady state values of the output might be impossible to calculate. For the simulations where the controlled process was stable, the steady-state values of the outputs were calculated as the average of all the collected data points between simulation times of 300 and 400 hours after the initial change in the inputs. Unstable combinations of inputs usually led to the process violating one of the shutdown limits given in the initial definition of the process (Downs and Vogel, 1993). Unstable conditions were naturally found to occur at the boundaries of the design space, and we observed that using a larger number of inputs often required us to limit the size of the input ranges further. This issue clearly points to the need of designing plant-wide control structures whose stability characteristics are more robust to changes in the operating point of the process represented by changes in the values of the inputs.

3.3. Model accuracy and response surface models

The normalized root mean-square error (NRMSE) and the ranges of the outputs are presented in Table 2. The NRMSE is calculated using the prediction error of the surrogate model against 1000 cross-validation simulations as defined above. The quadratic and cubic models in Eqs. (3) and (4) initially contained 55 and 220 parameters, respectively. The number of data points used in the estimation of these parameters were 165 for the quadratic design and 660 for the cubic design, about three times the number of parameters to be estimated. For both models, the amount of data used in parameter estimation was chosen to be sizably larger than the number of parameters in order to limit potential overfitting. This is a rather conservative approach and one needs not adhere to it if the detailed simulations are time-consuming to perform.

Please cite this article as: A.P. Tran, C. Georgakis, On the estimation of high-dimensional surrogate models of steady-state of plant-wide processes characteristics, Computers and Chemical Engineering (2018), https://doi.org/10.1016/j.compchemeng.2018.02.014

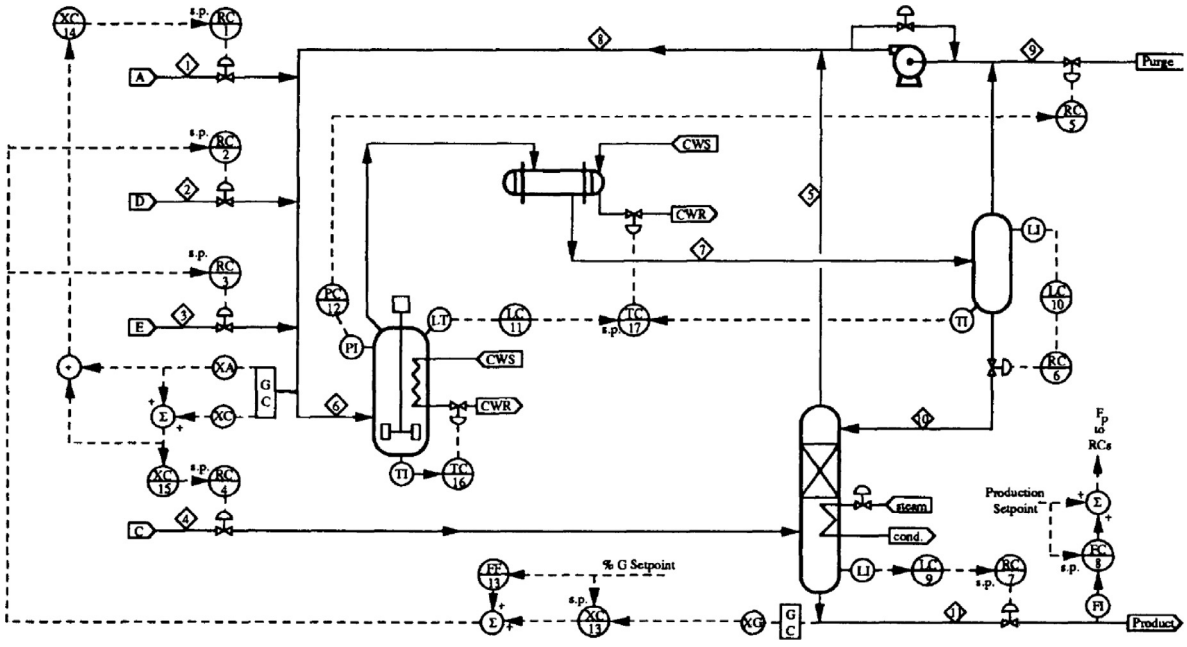

Fig. 1. The Tennessee Eastman process and its control structure. [From Downs and Vogel, 1993].

Table 1
Ranges for the inputs varied in terms of coded variables for the TE process.

Controller Set points		−1	0	+1
Production Rate	u_1	20.5 m^3/h	22.25 m^3/h	24.0 m^3/h
Stripper Level	u_2	40%	50%	60%
Separator Level	u_3	40%	50%	60%
Reactor Level	u_4	60%	65%	70%
Reactor Pressure	u_5	2600 kPa	2725 kPa	2850 kPa
Mole fraction G in Product	u_6	0.51	0.54	0.57
A Feed Mole Fraction in Reactor Feed	u_7	0.61	0.645	0.68
A + C Feed Mole Fraction in Reactor Feed	u_8	0.45	0.50	0.55
Reactor Temperature	u_9	119.5 °C	123 °C	126.5 °C

Table 2
Range, accuracy and model description of the surrogate models for the TE process.

Outputs	Units	Range		Quadratic RSMs			Third-order RSMs			
				NRMSE (%)	Terms		NRMSE (%)	Terms		
		Min	Max		1st	2nd		1st	2nd	3rd
Product D Mole Fraction		0.0015	0.105	4.04	2	22	1.64	3	22	71
Product E Mole Fraction		0.163	4.728	2.31	2	23	1.43	3	24	64
Product F Mole Fraction		0.0756	0.468	0.67	5	22	0.77	4	13	30
Product H Mole Fraction		37.8	47.2	1.53	5	20	0.83	4	8	23
Recycle Flow	kscmh	25.15	37.8	0.84	4	10	0.85	4	8	9
Reactor Feed Rate	kscmh	40.71	52.49	0.78	5	6	0.81	5	7	13
Purge Rate	kscmh	0.147	0.527	3.40	5	24	1.34	6	21	71
Product Separator Temperature	°C	76.03	105.2	0.78	4	6	1.04	4	6	8
Product Separator Pressure	kPa g	2507	2755	0.80	1	0	1.11	1	0	1
Product Separator Underflow	m^3/h	21.57	32.66	1.25	3	20	1.15	3	12	23
Stripper Pressure	kPa g	3095	3399	0.82	2	0	1.28	2	0	1
Stripper Underflow	m^3/h	20.5	24	0.84	1	0	0.84	1	0	0
Stripper Temperature	°C	46.56	77.61	0.92	6	22	1.01	4	8	27
Stripper Steam Flow	kg/h	−0.039	0.037	14.82	3	23	14.82	5	24	81
Compressor Work	kW	212.1	313.9	0.86	4	9	0.92	4	8	8
Reactor Cooling Water Outlet Temperature	°C	97.52	108.6	0.88	2	1	0.83	2	1	3
Separator Cooling Water Outlet Temperature	°C	64.01	105.6	0.95	6	18	0.79	5	8	29
Reactor Feed Mole Fraction B		27.44	37.41	0.57	2	1	0.86	2	1	2
Reactor Feed Mole Fraction D		5.479	19.73	1.56	3	19	1.08	2	12	24
Reactor Feed Mole Fraction E		14.4	21.46	0.54	1	0	0.97	1	0	1
Reactor Feed Mole Fraction F		4.639	8.978	0.87	3	20	0.53	3	10	13
Feed A Flowrate	kscmh	0.218	0.372	2.38	5	26	1.29	6	16	75
Feed D Flowrate	kg/h	3051	4211	0.96	3	2	1.03	3	2	7
Feed E Flowrate	kg/h	3660	5458	1.07	3	21	0.93	2	13	23
Feed A and C Flowrate	kscmh	8.145	9.853	0.69	3	2	1.16	3	1	8
Operating Cost	$/h	90.4	414.7	3.84	3	25	1.13	5	22	70

Please cite this article as: A.P. Tran, C. Georgakis, On the estimation of high-dimensional surrogate models of steady-state of plant-wide processes characteristics, Computers and Chemical Engineering (2018), https://doi.org/10.1016/j.compchemeng.2018.02.014

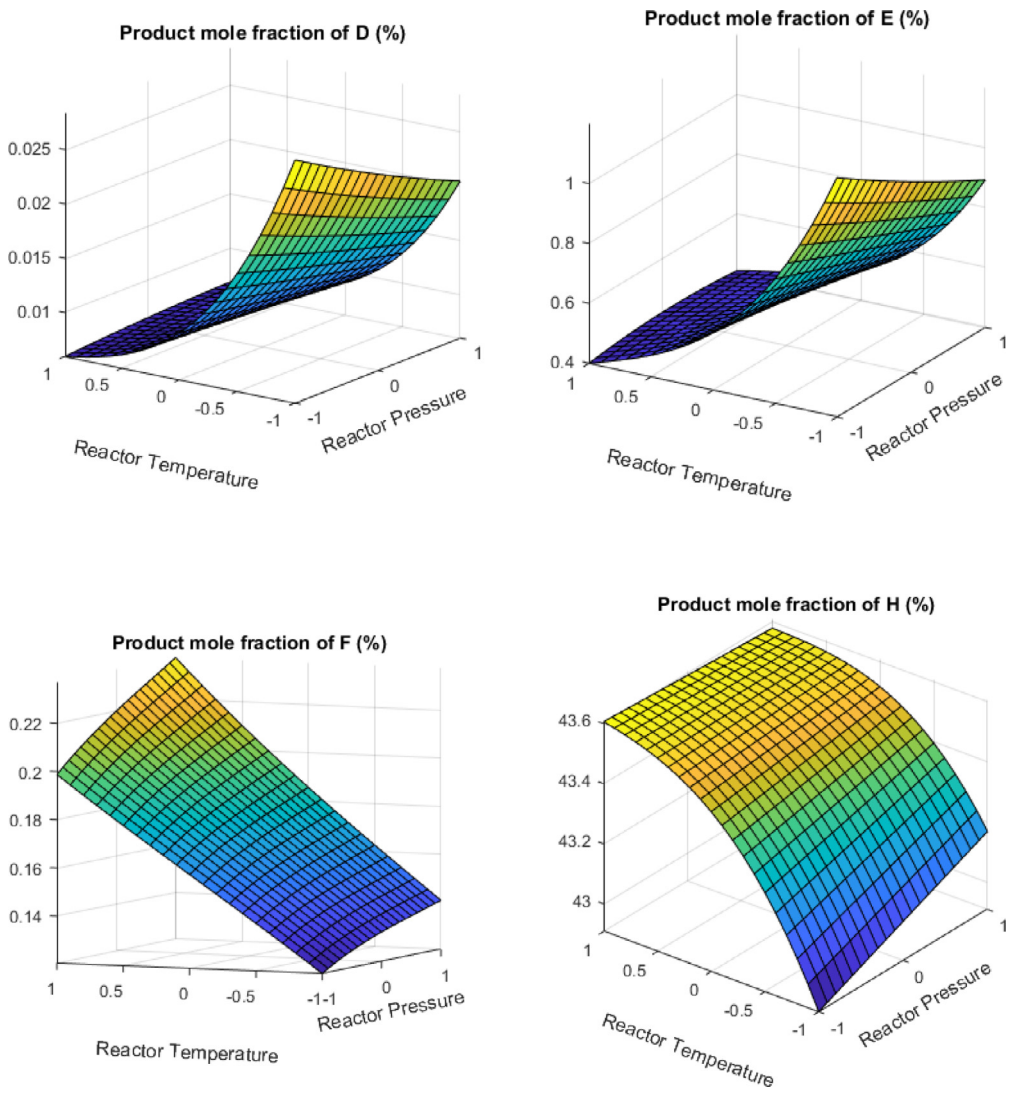

Fig. 2. Response surface models for the Tennessee Eastman process using the fitted cubic models. In all cases, the reactor pressure (u_5) and temperature (u_9) were varied. The other inputs were fixed at: $u_1 = 0.815$, $u_2 = 0.906$, $u_3 = 0.127$, $u_4 = 0.913$, $u_6 = 0.098$, $u_7 = 0.278$ and $u_8 = 0.547$.

To determine whether a quadratic model is sufficiently accurate, we compare its cross-validation NRMSE to that of the cubic model. By such comparisons of the corresponding two values given in Table 2, we can see that not all outputs benefit from the additional terms in the cubic model. The input-output relationships of relatively low complexity such as of the product separator temperature, reactor feed rate, stripper pressure and underflow, and Feed D flowrate show virtually no accuracy gain from developing a third-order RSM. These quadratic models had cross-validation errors about 1% or less. The net-elastic regularization removes most of the extra terms introduced in the cubic RSM as insignificant. For more complex input-output relationships, such as those for the product D mole fraction, purge rate, feed A flowrate and operating cost, the NRMSE error was reduced by about a factor of 2 from a quadratic to a cubic model. Outputs located upstream of the process tend to exhibit a lower model complexity and required less terms to reach a similar level of accuracy. However, since all the output measurements are collected at once, the required number of detailed simulations will often be determined by the most complex relationships to be modeled. In Fig. 2, the response surface models for the effects of the reactor temperature and the reactor pressure on the mole fractions of D, E, F and H are shown when the other inputs are at their reference values.

3.4. Model inversion and optimization using surrogate models

The polynomial form of the surrogate models naturally allows fast evaluations of values for the process outputs for a given value of the process inputs. It also enables the calculation of the necessary input values to achieve a desired set of output values. This only involves the solution of a set of nonlinear algebraic equations of polynomial complexity, a much less challenging task than the same calculation through the detailed knowledge-driven model. In addition, one can easily calculate important input-output relations such as the Hessian and Jacobian matrices which are difficult or impossible to calculate with the knowledge-driven models. Similarly, challenging optimization problems can be solved much more rapidly using a surrogate model compared to the detailed model.

For example, the production rate (u_1) and the mole fraction of G in the product (u_6) for the Tennessee Eastman process can be fixed and an optimal operating condition can be calculated that will minimize the operating cost. Substituting the zero value for u_1 and u_6 in the metamodel calculating the operating cost (last row in Table 2) and setting the [−1,1] range as a constraint for all the other inputs, a solution is easily derived using the interior point option in the *fmincon* function in MatLab. Convergence was found after 8 iterations and the results are presented in Table 3.

Please cite this article as: A.P. Tran, C. Georgakis, On the estimation of high-dimensional surrogate models of steady-state of plant-wide processes characteristics, Computers and Chemical Engineering (2018), https://doi.org/10.1016/j.compchemeng.2018.02.014

Table 3
Calculated optimal conditions for the TE process given a production rate of 22.25 m^3/h and mole fraction G in the product stream of 0.54.

Controller Set points		Coded values	Process values
Stripper Level	u_2	−1	40%
Separator Level	u_3	−1	40%
Reactor Level	u_4	−1	60%
Reactor Pressure	u_5	1	2850 kPa
A Feed Mole Fraction in Reactor Feed	u_7	0.3606	0.658
A + C Feed Mole Fraction in Reactor Feed	u_8	−0.0783	0.496
Reactor Temperature	u_9	−0.340	121.8 °C

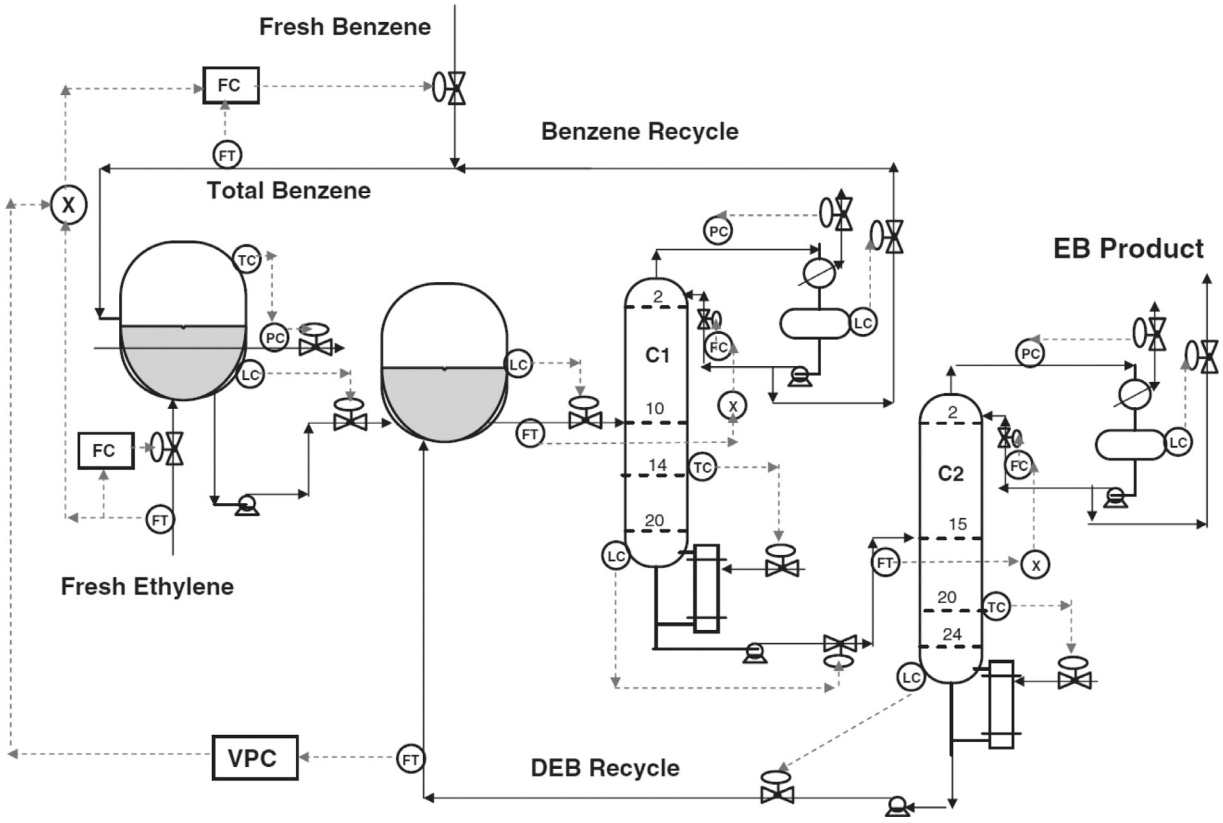

Fig. 3. Ethyl benzene process and its control structure [From Luyben, 2012].

Table 4
Ranges for the inputs varied in terms of coded variables for the EB process.

Controller Set points		−1	0	+1
DEB Recycle Flow(VPC)	u_1	230.21 kmol/h	242.71 kmol/h	255.21 kmol/h
Stage 14 Temp in Column 1	u_2	88.65 °C	93.15 °C	97.65 °C
Stage 20 Temp in Column 2	u_3	116.35 °C	120.35 °C	124.35 °C
1st Reactor Temp	u_4	163.57 °C	166.07 °C	168.57 °C
Fresh Etylene Feed	u_5	608.6 kmol/h	622.6 kmol/h	636.6 kmol/h
Liquid Level Reactor 1	u_6	4.7 m^2	4.95 m^2	5.2 m^2
Liquid Level Reactor 2	u_7	5.06 m^2	5.26 m^2	5.46 m^2

The procedure was repeated a few times with multiple starting points to verify that the calculated minimum is indeed the global minimum within the constraints of the input space. The discrepancy is expected to be the one listed in Table 2 with an estimated NRMSE of 1.13%, giving the average deviation from the simulation value. While such calculations are not expected to always coincide exactly with the global minimum from the original simulation, one can use this as the initial point to a global optimization algorithm in combination with the estimated Jacobian from the derived metamodels for accelerated convergence. Given the data-driven approach, the quantity and quality of the sample points is of importance on determining whether this initial point approaches a global extremum.

4. Ethyl Benzene (EB) process

4.1. Process description

Recently, the dynamic simulations of a series of industrial size processes along with the corresponding plant-wide control structures have been made available in a book about plant-wide control (Luyben, 2012). The related Aspen Dynamics software are available

Table 5
Range, accuracy and model description of the surrogate models for the EB process.

Outputs	Units	Range		Quadratic RSMs			Third-order RSMs			
				NRMSE (%)	Terms by order		NRMSE (%)	Terms by order		
		Min	Max		1st	2nd		1st	2nd	3rd
First Reactor Heat Duty	GJ/h	−39.22	−35.61	0.71	1	17	0.84	1	13	4
C1 Condenser Heaty Duty	GJ/h	−57.97	−44.16	0.77	5	4	0.78	5	4	9
C1 Reboiler Heat Duty	GJ/h	19.69	28.69	0.83	2	13	0.85	2	11	7
C2 Condenser Heat Duty	GJ/h	−42.16	−39.82	0.68	1	2	0.64	1	1	1
C2 Reboiler Heat Duty	GJ/h	34.62	36.97	0.42	5	3	0.67	5	3	11
DEB Recycle Stream DEB Comp.		0.99815	0.99955	1.01	1	1	1.13	1	1	1
Reactor 2 Stream Out Flowrate	kmol/h	1545	1887	0.85	2	12	0.88	2	9	5
Reactor 2 Stream out B Comp.		0.4144	0.5375	0.79	2	4	0.76	2	4	2
Reactor 2 Stream out DEB Comp.		0.1220	0.1654	0.71	5	1	0.55	5	1	1
Reactor 2 Stream out EB Comp.		2.537E−05	4.644E−05	0.85	3	4	0.93	3	4	4
Benz. Recycle Flowrate	kmol/h	678.4	1020.0	0.88	2	13	0.81	2	10	6
Benz. Recycle Stream B. Comp.		0.93102	0.99675	0.75	1	3	0.66	1	3	0
Fresh Benzene Feed	kmol/h	608.3	638.4	0.74	2	0	1.42	2	0	8
Product Stream Flowrate	kmol/h	608.3	638.4	0.74	2	0	1.58	2	0	8
Product Stream B Comp.		2.305E−04	4.679E−03	2.32	5	15	0.91	4	15	38
Product Stream DEB Comp.		3.443E−04	7.154E−04	4.27	3	8	1.46	3	6	19
Product Stream EB Comp.		0.99473	0.99934	2.02	2	13	0.79	2	12	30

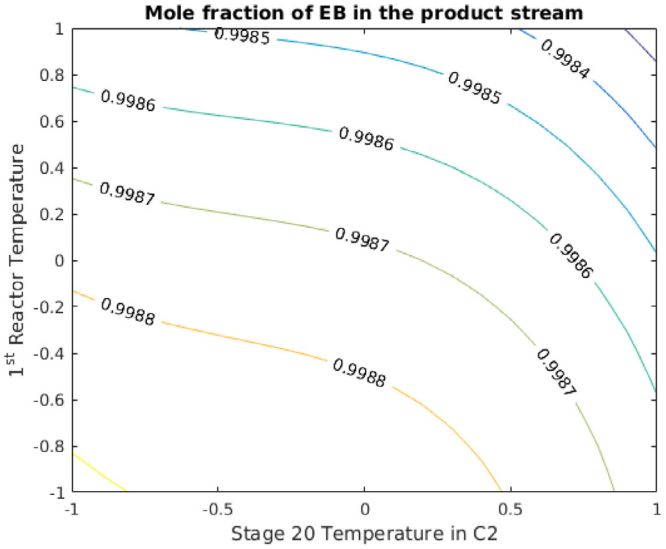

Fig. 4. Contour plot for EB mole fraction in the product stream using the fitted cubic models by varying u_3 and u_4. The other inputs are kept at a coded value of 0.

from the book's author. A control structure, composed of multiple SISO controllers, is implemented in each of these simulations.

T production of ethyl benzene is achieved via a reaction involving benzene and ethylene. A byproduct in the form of diethyl benzene is formed in the process, but can be recycled to react with the excess of benzene to form the desired ethyl benzene. The reactions are given as:

$$\begin{aligned} C_2H_4 + C_6H_6 &\rightarrow C_8H_{10} \\ C_8H_{10} + C_2H_4 &\rightarrow C_{10}H_{14} \\ C_{10}H_{14} + C_6H_6 &\rightarrow 2C_8H_{10} \end{aligned} \tag{9}$$

All three reactions are irreversible and the reaction rates depend linearly on the concentration of each of the two reactants. The activation energy of the second reaction is the highest. Therefore a lower reactor temperature improves the selectivity towards the desired ethyl benzene.

The process flowsheet is shown in Fig. 3 along with its control structure. There are two feed streams for fresh benzene and ethylene, and a single stream out containing mostly the desired product ethyl benzene. The components are referred to as B for benzene, E for ethylene, EB for ethyl benzene and DEB for diethyl benzene. The fresh benzene combines with the recycled benzene and fresh ethylene to be fed to the first CSTR reactor, with the reaction temperature controlled by a steam valve. The product of the first reactor is then fed to the second CSTR reactor to react with the DEB recycle stream. The high amount of unreacted benzene and low amount of ethylene promotes the reaction of DEB into the desired EB product. The first distillation column separates the lighter B, while the second distillation column separates the desired EB from DEB. The two CSTRs, two distillation columns and two recycle streams make this process highly interactive and nonlinear. In addition, this process exhibits the snowball effect, where small disturbances in one part of the process lead to large changes in the recycle flowrate(s) (Luyben, 1994). The valve position controller (VPC) was placed to ensure that the changes in DEB recycle stay modest by adjusting the amount of fresh B fed to the process.

4.2. Design of the surrogate models

The set-point values for the seven controlled variables that were used as inputs for the surrogate model are listed in Table 4. The VPC and all the liquid level controllers in the process were originally proportional-only. Due to difficulties in obtaining convergent steady-state values, an integral element was added with $\tau_I = 300$ min for all the liquid levels and $\tau_I = 1200$ min for the VPC controller. There are six additional controllers for which the set-points were not changed: the liquid level controllers in the two reboilers and the two condensers, and the two pressure controllers in the columns. The pressures were kept at the minimum values for which water could be used in the condenser. The liquid levels in the columns had a lesser impact than the seven inputs for which the RSMs were built. The time after which steady-state data were collected was 400 hours since changes occurred. This is the time after which the flowrate of fresh benzene is expected to be equal to the flowrate of product coming out of the process. The control structure used in this process is highly sensitive to changes in flowrates and liquid levels in the reactors, which leads to the narrow ranges over which one could vary the selected inputs without causing a dynamic instability. The quadratic and cubic RSM models, described by Eqs. (3) and (4), had 36 and 120 initial parameters to be estimated respectively. The corresponding number of simulations were 108 for the quadratic models and 360 for the third-order models.

Please cite this article as: A.P. Tran, C. Georgakis, On the estimation of high-dimensional surrogate models of steady-state of plant-wide processes characteristics, Computers and Chemical Engineering (2018), https://doi.org/10.1016/j.compchemeng.2018.02.014

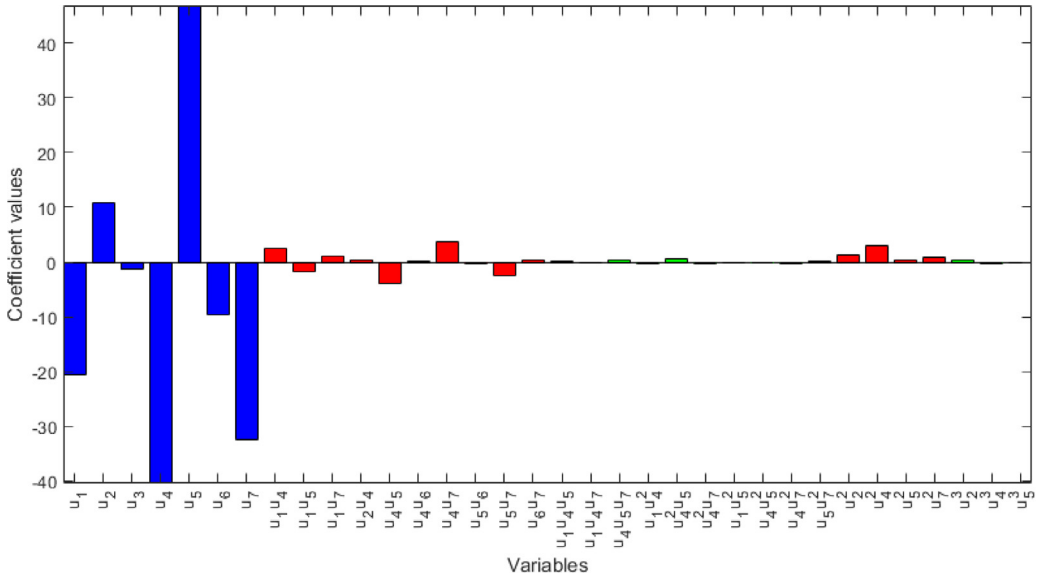

Fig. 5. Coefficient values for the recycle flowrate metamodel for the ethyl benzene process. (blue = linear terms, red = quadratic terms, green = cubic terms, units = kmol/h). (For interpretation of the references to colour in this figure legend, the reader is referred to the web version of this article.)

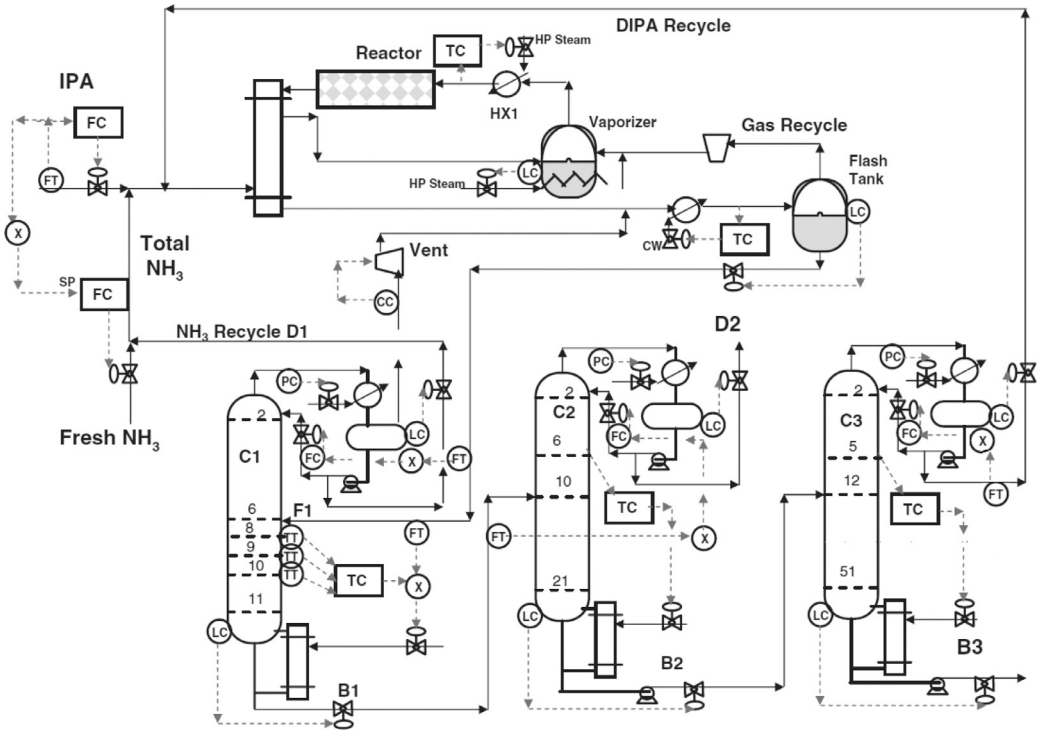

Fig. 6. MIPA process and its control structure [From Luyben, 2012].

4.3. Model accuracy and response surface models

The NRSME of the quadratic RSMs was less than 1% for most of the outputs listed in Table 5, with the exception of the product stream compositions. For these cases, the third order terms helped reduce the NRSME by a factor greater than 2. Even though there were initially 120 possible terms in the third-order RSMs, most of the estimated surrogate models have fewer than 20 terms. Because the process is highly multivariable and nonlinear and the control structure used is linear, it was difficult to find a large seven-dimensional hypercube in the input space where all operating points lead to stable steady states. The domain in the input space with stable steady states was narrower than the desired ranges for each of the inputs. Consequently, some input-output relationships were accurately described by very simple and often linear models. In Fig. 4, we show the possibility of using metamodels to delineate desired regions using contour plots. These contour plots are not easy to calculate through the detailed model, yet they are easily obtained through the metamodels.

4.4. Snowball effect in the Ethyl Benzene process

The magnitude of the parameters in the metamodel for the benzene recycle flowrate is presented in a bar chart in Fig. 5. The constant coefficient value of 823.00 kmol/h was omitted for visu-

Table 6
Ranges for the inputs varied in terms of coded variables for the MIPA process.

Controller Variable		−1	0	+1
Avg. Temp. Ammonia Column (C1)	u_1	132 °C	137 °C	142 °C
Temperature Product Column (C2)	u_2	61 °C	65 °C	69 °C
Temperature Recycle Column (C3)	u_3	57 °C	61 °C	65 °C
DIPA Comp. in Recycle Column (C3)	u_4	0.038	0.0425	0.047
Fresh IPA Feed	u_5	42 kmol/h	45 kmol/h	48 kmol/h
Reactor Temperature	u_6	157.5 °C	159 °C	160.5 °C
Comp. H2 Vent	u_7	0.045	0.050	0.055

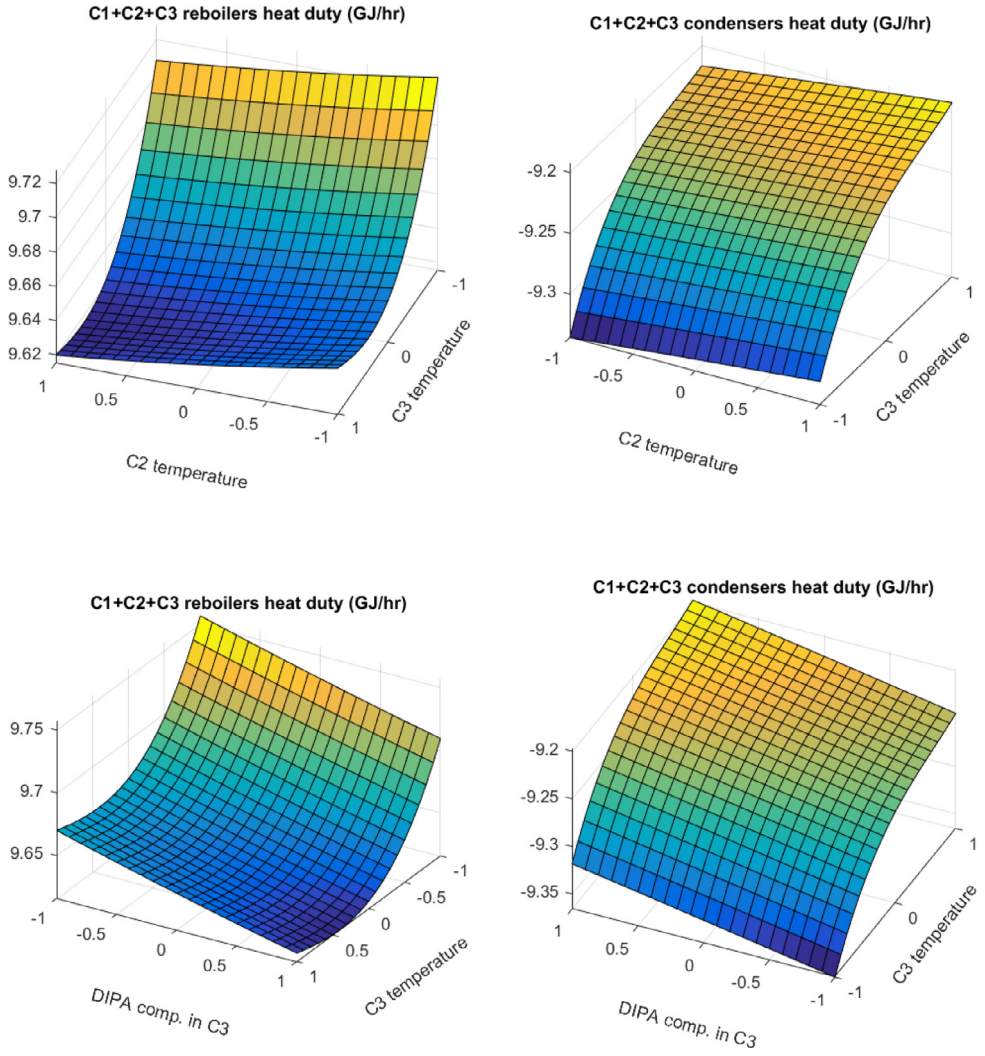

Fig. 7. Response surface models for the mono-isopropyl amine process using the fitted cubic models. In (a) and (b), the column 2 temperature (u_2) and the column 3 temperature (u_3) are varied. In (c) and (d), the column 3 temperature (u_3) and DIPA composition in the recycle column C3 (u_4). When fixed, the input values set at $u_1 = -0.488$, $u_2 = -0.243$, $u_4 = 0.571$, $u_5 = 0.596$, $u_6 = 0.581$ and $u_7 = 0.919$.

alization purposes. Luyben detailed that in processes with 2 recycle streams or more, the flowrate of each recycle stream should be fixed to prevent the snowball effect (Luyben, 1994). Since the benzene recycle flowrate was left as a free variable in this process, the factors contributing to an increase or decrease in this flowrate can be inferred from the developed surrogate model. The largest changes in this flow rate are caused by the linear terms with smaller contributions from the quadratic and 2-way interaction terms.

There is a balancing effect between the DEB recycle flowrate (u_1) and the benzene recycle flowrate. At steady-state, an increase in the bottom recycle stream of DEB leads to a reduction in benzene recycle flowrate. A higher reactor temperature (u_4) drives the desired reaction and leads to reduced benzene recycle flowrates. An increase in ethylene feed (u_5) leads, quite expectedly, to an increase in benzene recycle flowrate and vice-versa. One might note that the liquid levels (u_6 and u_7) are not fixed in this control structure, as these variables were controlled by proportional-only controllers. However, lowering the liquid levels in the reactors, and in the second one in particular, can significantly reduce the recycled benzene, leading to potential energy cost savings. This must be counterbalanced by the possible changes in the conversion at the exit of the second reactor. These observations, so clearly deduced from the metamodel, would have been most challenging to observe from the detailed model.

Please cite this article as: A.P. Tran, C. Georgakis, On the estimation of high-dimensional surrogate models of steady-state of plant-wide processes characteristics, Computers and Chemical Engineering (2018), https://doi.org/10.1016/j.compchemeng.2018.02.014

Table 7
Range, accuracy and model description of the surrogate models for the MIPA Process.

Outputs	Units	Range		Quadratic RSMs			Third-order RSMs			
				NRMSE (%)	Terms		NRMSE (%)	Terms		
		Min	Max		1st	2nd		1st	2nd	3rd
Product Stream Flowrate	kmol/h	41.84	47.92	0.84	1	0	1.59	1	0	1
Product Stream DIPA Comp.		2.502E−04	7.627E−04	0.74	2	3	1.40	2	2	6
Product Stream MIPA Comp.		9.985E−01	9.995E−01	0.93	2	1	1.93	3	6	8
Product Stream NH_3 Comp.		2.757E−04	7.409E−04	1.47	2	2	3.97	2	5	12
Ammonia Feed Flowrate	kmol/h	41.91	47.97	0.84	1	0	1.32	1	0	1
Water Stream Flowrate	kmol/h	42.04	48.09	0.84	1	0	1.71	1	0	1
Water Stream Water Comp.		9.982E−01	9.990E−01	1.46	3	4	1.06	2	4	5
Column 1 Feed Flowrate	kmol/h	188.2	220.9	1.34	2	1	1.18	2	1	2
Column 1 Feed DIPA Comp.		0.08763	0.09353	1.30	3	8	0.89	3	7	13
Column 1 Feed MIPA Comp.		2.185E−01	2.234E−01	1.28	2	8	0.61	2	7	5
Column 1 Feed NH3 Comp.		0.4524	0.4638	2.41	3	10	0.83	3	8	9
Column 1 Feed Water Comp.		0.2212	0.2317	2.37	4	5	0.74	4	4	7
Column 1 Distillate Flow Rate	kmol/h	84.02	96.11	0.84	1	0	0.85	1	0	0
Column 1 Distillate NH3 Comp.		9.986E−01	9.992E−01	0.70	4	5	3.85	4	12	23
Vent Stream Flowrate	kmol/h	2.660	5.236	1.67	3	4	1.31	2	4	4
Vent Stream NH_3 Comp.		0.9449	0.9549	0.83	0	0	0.84	0	0	0
DIPA Recycle Flowrate	kmol/h	17.44	24.05	2.12	5	10	0.92	5	8	13
DIPA Recycle DIPA Comp.		0.8241	0.9753	2.82	2	5	1.23	2	5	5
Gas Recycle Flowrate	kmol/h	12.08	15.39	0.90	2	3	1.15	2	3	1
Gas Recycle H_2 Comp.		0.5107	0.6884	1.38	3	1	1.78	3	1	8
Gas Recycle MIPA Comp.		0.01246	0.02202	0.92	1	0	0.93	1	0	0
Gas Recycle NH_3 Comp.		0.2977	0.4642	1.33	2	0	1.36	2	0	1
K2 Power	GJ/h	0.4031	0.8732	1.66	3	4	1.37	3	4	7
Heat Exchanger 1 Heat Duty	GJ/h	0.004018	0.093450	1.34	3	4	0.59	3	4	5
Heat Exchanger 2 Heat Duty	GJ/h	−2.792	−1.708	1.38	3	2	1.54	3	0	1
FEHE Heat Duty	GJ/h	4.912	5.543	0.94	4	2	0.83	4	2	6
Condenser Column 1 HD	GJ/h	−2.384	−2.066	0.85	0	0	1.20	0	0	0
Reboiler Column 1 HD	GJ/h	4.473	5.748	1.46	3	3	1.54	3	3	7
Condenser Column 2 HD	GJ/h	−3.374	−2.893	1.19	1	1	1.73	2	1	1
Reboiler Column 2 HD	GJ/h	0.949	1.115	1.14	2	0	0.92	2	0	0
Condenser Column 3 HD	GJ/h	−3.965	−3.189	1.43	3	4	1.15	3	4	3
Reboiler Column 3 HD	GJ/h	2.753	3.466	1.42	2	2	1.33	2	2	8
Vaporizer HD	GJ/h	0.975	1.556	1.60	3	1	1.10	4	1	3

5. Mono-Isopropyl Amine (MIPA) process

5.1. Process description

This process involves the formation of mono-isopropyl amine (MIPA) from ammonia and isopropanol (IPA) (Luyben, 2012). Similarly, to the ethyl benzene process, an undesired product in the form of di-isopropyl amine (DIPA) is formed and can be recycled to form MIPA in the presence of ammonia. The three reactions are given as:

$$\begin{aligned} IPA + NH_3 &\rightarrow MIPA + H_2O \\ IPA + MIPA &\rightarrow DIPA + H_2O \\ DIPA + NH_3 &\rightleftharpoons 2MIPA \end{aligned} \tag{10}$$

The first two reactions are irreversible and the third reaction is reversible. In order to avoid the formation of byproduct DIPA, the MIPA concentration needs to be low while the concentration of ammonium should be maintained at a high value. The activation energy for the MIPA reaction is smaller than that for the DIPA reaction, thus a low temperature favors the desired reaction. H_2 is circulated around the process to improve catalyst life, but does not participate in the reaction. Water is also formed and needs to be separated from the product stream.

The process flowsheet is shown in Fig. 6 along with its control structure. There are two feed streams to supply IPA and ammonia and two exit streams for the desired product (D2) and water (B2). DIPA and ammonia recycle streams are combined with the fresh feeds and the stream is then heated through a feed-effluent heat exchanger (FEHE) that recovers energy from the exit stream of the tubular reactor. This combined stream is vaporized with the gas recycle stream from the flash tank. The vaporized stream is then adjusted to the desired reaction temperature in heat exchanger 1. After the reaction, the reactor outlet stream is cooled down through the FEHE and the temperature is adjusted further with heat exchanger 2 before being fed to a flash tank from which the liquid phase is separated in a series of three distillation columns. In the first column, the distillate is the lighter ammonia that is being recycled. A vent stream, containing mostly H_2 and NH_3, is also used to remove gas from the reflux drum to avoid hydrogen suppression of the condenser temperature. The bottom of column 1 is then fed to column 2 from which the distillate contains the desired product MIPA. Column 3 is used to separate the remaining DIPA from water. The separation between DIPA and water is particularly difficult and requires 52 stages. A high-pressure of 333 psia is used in column 1 due to the low boiling point of ammonia and the use of water in the condenser. The pressures in columns 2 and 3 are 30 and 5 psia, respectively.

5.2. Design of the surrogate models

Seven of the controller set points were varied as inputs and are listed in Table 6. The liquid level and pressure set points in all three columns were kept constant. The simulation time after which the steady-state values were collected was 400 hours after the initial changes were introduced. Unstable combinations of inputs often led to the failure of heat exchanger 1 to control the temperature of the feed to the reactor. This is due to the complex heat integration scheme around the reactor, which led to the small ranges over which the fresh IPA feed and reactor temperature were varied.

Please cite this article as: A.P. Tran, C. Georgakis, On the estimation of high-dimensional surrogate models of steady-state of plant-wide processes characteristics, Computers and Chemical Engineering (2018), https://doi.org/10.1016/j.compchemeng.2018.02.014

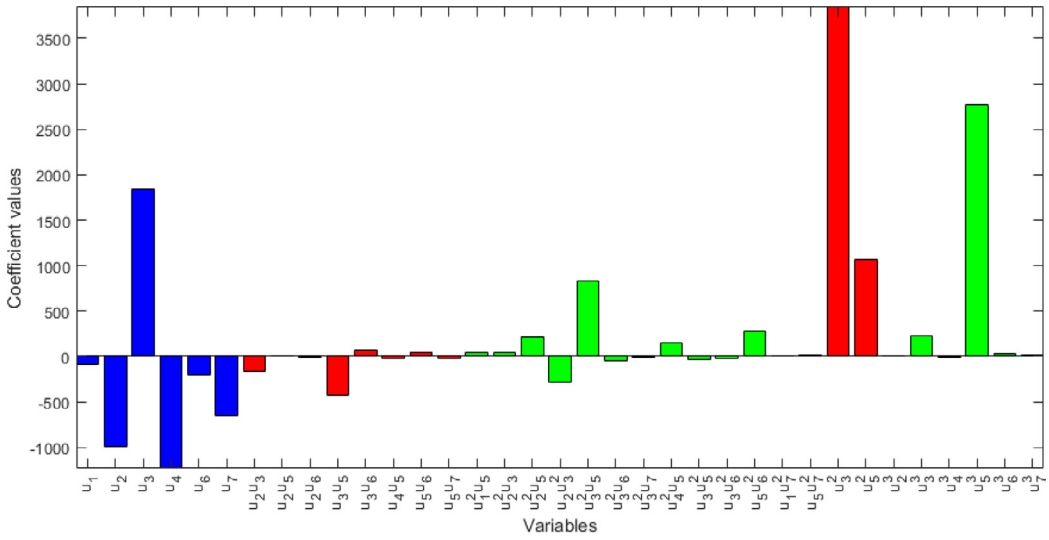

Fig. 8. Coefficient values for the recycle flowrate metamodel for the ethyl benzene process. Omitted are the constant coefficient = $7.66^{*}10^{5}$ and the coefficient for $u_5 = 7.59^{*}10^{4}$ (units = \$/year).

5.3. Model accuracy and response surface models

Similarly to the ethyl benzene process, the third-order RSMs brought higher accuracy for most of the output variables. The models are relatively simple when compared to the ones developed for the Tennessee Eastman process. An important limitation to the development of accurate surrogate models resides in the stability of the control structure used in this process. It is likely that an improvement in the control structure and a better description of the feasible input regions will lead to more practical surrogate models encompassing larger operating ranges. In Fig. 7, the effects on the condenser and the reboiler heat duties caused by changes in the controller temperatures in C2 and C3, as well as the DIPA composition in C3 are shown for a given process condition (Table 7).

5.4. Heat integration in the mono-isopropyl amine process

The output variables for the mono-isopropyl amine process that contributes to the energy costs of the plant are: the C1, C2, and C3 reboilers, the vaporizer and the first heat exchanger. The FEHE (second heat exchanger) did not require steam inputs, and was thus omitted from energy cost calculations in the original plant design (Luyben, 2012). The vaporizer, C1 reboiler and first heat exchanger all use high-pressure steam which is priced at \$9.83/GJ. The C2 and C3 reboilers make use of low-pressure steam with a pricing of \$6.08/GJ. Combining these steam costs and the calculated surrogate models yields the cubic model shown in Fig. 8.

The fresh IPA feed flowrate (u_5) has by far the greatest impact on the energy costs in this process with large linear, quadratic and cubic terms. This is an expected outcome since it has the most direct impact on the levels of production. Increasing the separation temperature in the product column C2 (u_2) decreases the amount to be separated in column 3, and leads to a decrease in energy costs. Lowering the column C3 temperature (u_3) allows important cost savings from the linear u_3, quadratic u_3^2 and interaction $u_3^2u_5$ terms. The decrease in hydrogen composition in the vent stream (u_6) and DIPA composition in the recycle column C3 (u_4) can also impact energy savings. The latter observation is best understood by focusing on the control structure, as the Stage 31 DIPA composition is used to regulate the reboiler heat duty of the column C3.

6. Conclusions

The methodology that was initially introduced in Georgakis and Li (2010) is improved and further tested against a larger number of inputs in the original TE process and against two additional processes of comparable complexity. It is proven to be very successful in the estimation of accurate steady-state surrogate models for plant-wide chemical processes. Net-elastic regularization is introduced as an alternative regression method in order to reduce the model complexity and alleviate potential overfitting issues. We have shown that such methods can provide faster parameter estimation for the model compared to stepwise regression. For the quadratic models, the number of linear and nonlinear terms examined were 55, 36 and 36 for the three processes. For the cubic models, the corresponding numbers of terms examined are 220, 120 and 120. The number of outputs modeled are 26, 17 and 33 for the three processes, resulting in a total of 76 models estimated. For one of the processes, the net-elastic regularization results in models that have as few as 1 term and as many as 31 terms of the possible 55 in a quadratic model. The corresponding numbers for a cubic model of the same process were as few as 1 and as many as 110. Similar numbers were observed in the other two processes. D-optimal designs were used to select the input values for the detailed simulations in all cases examined. The cross-validation errors of the metamodels obtained from the data for the cubic designs were less than 2% in NRMSE values.

Several examples of the use of these surrogate models were also presented. They include calculations and arguments about the heat integration in the MIPA process, the snowball effects for the EB process, and insights into the cost optimization in the TE process. The polynomial form of the metamodels allows for the easy calculation of the Jacobian and Hessian functions around a given steady state. This was used in the optimization task of the Tennessee Eastman process.

While the accuracy of the developed surrogate models is particularly high, there remain important challenges to be addressed. The main limitation that we encountered was related to the identification of stable steady-state data points over a large high-dimensional input space. This can be overcome by using the steady state plant-wide model (instead of the dynamic model used here) to bypass the stability challenges that we faced with the current control structure. This challenge is a strong indicator of the need

Please cite this article as: A.P. Tran, C. Georgakis, On the estimation of high-dimensional surrogate models of steady-state of plant-wide processes characteristics, Computers and Chemical Engineering (2018), https://doi.org/10.1016/j.compchemeng.2018.02.014

for more robust plant-wide control structures that enable operation over wider process windows. The development of similar metamodels for the open-loop steady state and dynamic characteristics of the process, with most of the controllers removed, could greatly facilitate the design of more effective multivariable and nonlinear plant-wide controllers, which are able to stably operate the process over a wider operating region.

Acknowledgments

The authors would like to acknowledge Dr. William L. Luyben for providing the simulations of the ethylene benzene and monoisopropyl amine processes used in this paper.

References

Banerjee, I., Ierapetritou, M., 2006. An adaptive reduction scheme to model reactive flow. Combust. Flame 144, 619–633. doi:10.1016/j.combustflame.2005.10.001.
Bathelt, A., Ricker, N.L., Jelali, M., 2015. Revision of the Tennessee eastman process model. In: IFAC-PapersOnLine, pp. 309–314. doi:10.1016/j.ifacol.2015.08.199.
Bhosekar, A., Ierapetritou, M., 2017. Advances in surrogate based modeling, feasibility analysis and and optimization: a review. Comput. Chem. Eng. 108, 250–267. doi:10.1016/j.compchemeng.2017.09.017.
Biegler, L.T., Zavala, V.M., 2009. Large-scale nonlinear programming using IPOPT: an integrating framework for enterprise-wide dynamic optimization. Comput. Chem. Eng. 33, 575–582. doi:10.1016/j.compchemeng.2008.08.006.
Boukouvala, F., Floudas, C.A., 2017. ARGONAUT: AlgoRithms for Global Optimization of coNstrAined grey-box compUTational problems. Optim. Lett. 11, 895–913. doi:10.1007/s11590-016-1028-2.
Boukouvala, F., Hasan, M.M.F., Floudas, C.A., 2017. Global optimization of general constrained grey-box models: new method and its application to constrained PDEs for pressure swing adsorption. J. Glob. Optim. 67, 3–42. doi:10.1007/s10898-015-0376-2.
Caballero, J.A., Grossmann, I.E., 2008. An algorithm for the use of surrogate models in modular flowsheet optimization. AIChE J 54, 2633–2650. doi:10.1002/aic.11579.
Cozad, A., Sahinidis, N.V., Miller, D.C., 2014. Learning surrogate models for simulation-based optimization. AIChE J 60, 2211–2227. doi:10.1002/aic.14418.
Downs, J.J., Vogel, E.F., 1993. A plant-wide industrial process control problem. Comput. Chem. Eng. 17, 245–255. doi:10.1016/0098-1354(93)80018-I.
Eason, J., Cremaschi, S., 2014. Adaptive sequential sampling for surrogate model generation with artificial neural networks. Comput. Chem. Eng. 68, 220–232. doi:10.1016/j.compchemeng.2014.05.021.
Fahmi, I., Cremaschi, S., 2012. Process synthesis of biodiesel production plant using artificial neural networks as the surrogate models. Comput. Chem. Eng. 46, 105–123. doi:10.1016/j.compchemeng.2012.06.006.
Georgakis, C., 2013. Design of dynamic experiments: a data-driven methodology for the optimization of time-varying processes. Ind. Eng. Chem. Res. 52, 12369–12382. doi:10.1021/ie3035114.
Georgakis, C., Li, L., 2010. On the calculation of operability sets of nonlinear high-dimensional processes. Ind. Eng. Chem. Res. 49, 8035–8047. doi:10.1021/ie1009316.
Henao, C.A., Maravelias, C.T., 2010. Surrogate-Based Process Synthesis 7946, 1129–1134. doi:10.1016/S1570-7946(10)28189-0.
Jin, R., Chen, W., Simpson, T.W., 2001. Comparative studies of metamodelling techniques under multiple modelling criteria. Struct. Multidiscip. Optim. 23, 1–13. doi:10.1007/s00158-001-0160-4.
Klebanov, N., Georgakis, C., 2016. Dynamic response surface models: a data-driven approach for the analysis of time-varying process outputs. Ind. Eng. Chem. Res. 55, 4022–4034. doi:10.1021/acs.iecr.5b03572.
Larsson, T., Hestetun, K., Hovland, E., Skogestad, S., 2001. Self-optimizing control of a large-scale plant: the Tennessee Eastman Process. Ind. Eng. Chem. Res. 40, 4889–4901. doi:10.1021/ie000586y.
Luyben, W.L., 2012. Principles and Case Studies of Simultaneous Design. John Wiley & Sons.
Luyben, W.L., 1994. Snowball effects in reactor/separator processes with recycle. Ind. Eng. Chem. Res. 33, 299–305.
Lyman, P.R., Georgakis, C., 1995. Plant-wide control of the Tennessee Eastman problem. Comput. Chem. Eng. 19, 321–331. doi:10.1016/0098-1354(94)00057-U.
Misener, R., Floudas, C.A., 2014. ANTIGONE: Algorithms for coNTinuous/integer global optimization of nonlinear equations. J. Glob. Optim. 59, 503–526. doi:10.1007/s10898-014-0166-2.
Müller, J., Shoemaker, C.A., 2014. Influence of ensemble surrogate models and sampling strategy on the solution quality of algorithms for computationally expensive black-box global optimization problems. J. Glob. Optim. 60, 123–144. doi:10.1007/s10898-014-0184-0.
Müller, J., Shoemaker, C.A., Piché, R., 2013. SO-MI: A surrogate model algorithm for computationally expensive nonlinear mixed-integer black-box global optimization problems. Comput. Oper. Res. 40, 1383–1400. doi:10.1016/j.cor.2012.08.022.
Noble, W.S., 2006. What is a support vector machine? Nat. Biotechnol 24, 1565–1567. doi:10.1038/nbt1206-1565.
Qian, J., Hastie, T., Friedman, J., Tibshirani, R., Simon, N., 2013 Glmnet for Matlab, 2013. URL http//www.stanford.edu/~Hast.
Ricker, N.L., 1996. Decentralized control of the Tennessee Eastman Challenge Process. J. Process Control 6, 205–221. doi:10.1016/0959-1524(96)00031-5.
Sahinidis, N.V., 1996. BARON: A general purpose global optimization software package. J. Glob. Optim. 8, 201–205. doi:10.1007/BF00138693.
Tibshirani, R., 1996. Regression selection and shrinkage via the Lasso. J. R. Stat. Soc. B doi:10.2307/2346178.
Wang, G.G., Shan, S., 2007. Review of metamodeling techniques in support of engineering design optimization. J. Mech. Des. 129, 370. doi:10.1115/1.2429697.
Zhang, Y., Sahinidis, N.V, 2012. Uncertainty quantification in CO2 sequestration using surrogate models from polynomial chaos expansion. Ind. Eng. Chem. Res. 52, 3121–3132. doi:10.1021/ie300856p.
Zou, H., Hastie, T., 2005. Regularization and variable selection via the elastic net. J. R. Stat. Soc. Ser. B Stat. Methodol. 67, 301–320. doi:10.1111/j.1467-9868.2005.00503.x.

Please cite this article as: A.P. Tran, C. Georgakis, On the estimation of high-dimensional surrogate models of steady-state of plant-wide processes characteristics, Computers and Chemical Engineering (2018), https://doi.org/10.1016/j.compchemeng.2018.02.014